Received 3 July 2025; Accepted 23 September 2025
https://doi.org/10.48612/letters/2025-4-256-262
https://elibrary.ru/mfplzh

The variation in the martensitic transformation during thermal cycling of the cast Ti-Hf-Ni-Cu shape memory alloys under or without stress

S. P. Belyaev[1], N. N. Resnina[†1], A. I. Bazlov[1,2], A. V. Sibirev[1], I. V. Ponikarova[1], R. M. Bikbaev[1], M. E. Trofimova[1], A. M. Ivanov[1]

[†]resnat@mail.ru

[1]Saint-Petersburg State University, Saint-Petersburg 199034, Russia
[2]National University of Science and Technology "MISIS", Moscow 119049, Russia

Abstract: This paper examines the variation in martensitic transformation temperatures during thermal cycling with or without constant stress. Five cast $Ti_{50.2-x}Hf_xNi_{49.8-y}Cu_y$ (x=1 or 9.5 at.%, y=1, 5 or 10 at.%) alloys with various chemical compositions were subjected to ten thermal cycles in stress-free state or under 100 MPa (for x=1 at.%) or 200 MPa (for x=9.5 at.%). It was found that during thermal cycling without stress, the transformation temperatures decreased in all alloys; however, the smallest variation was observed in the $Ti_{49.2}Hf_1Ni_{44.8}Cu_5$ and $Ti_{40.7}Hf_{9.5}Ni_{39.8}Cu_{10}$ alloys. Thermal cycling under stress showed that the variation in the transformation temperatures might be smaller or larger than on thermal cycling without stress. It was shown that an increase in the intensity of the variation in transformation temperatures on thermal cycling under stress did not depend on the chemical composition of the alloy, yield limit for dislocation slip or variation in the dislocation density. This showed that the variation in the dislocation density was not the main reason for the variation in the transformation temperatures during thermal cycling. It was concluded that the thermal cycling stability shown by the Ti-Hf-Ni-Cu alloys during thermal cycling without stress is not maintained during thermal cycling under stress.

Keywords: shape memory alloys, thermal cycling, NiTi-based alloys, martensitic transformation

Acknowledgements: *This study was supported by Russian Science Foundation (# 23-19-00280).*

1. Introduction

One of the wide applications of shape memory alloys is the repeat action devices, i. e., the actuator, where the strain variation repeats during cooling and heating through a temperature range of the martensitic transformations [1–2]. For the stable operation of such devices, the strain variation parameters such as transformation temperatures and strain should not change during thermal cycling. In other words, the shape memory alloys must demonstrate a high thermal cycling stability of the functional properties. At the same time, the NiTi-based alloys, which are the widely spread shape memory alloys for application, demonstrate weak thermal cycling stability [3–9]. It is known that the temperatures of the martensitic transformations decrease during thermal cycling [3–6], while the recoverable strain (the value of the shape memory effect) may increase (training effect) or decrease (degradation effect) depending on stress acting on cooling and heating [7–9]. A weak thermal cycling stability of the B2 ↔ B19' martensitic transformation is hardly dependent on the alloy composition, and this is observed in binary NiTi alloys [3–5, 7–9] as well as in ternary NiTi-X (X = Cu, Hf, Nb) [10–12] or quaternary Ni-X-Ti-Y (X = Cu, Y = Hf, Zr) alloys [13–16].

It is believed that the weak thermal cycling stability of the martensitic transformation can be mainly attributed to an increase in the dislocation density during repeating thermal cycling through a temperature range of the martensitic transformations [3–4, 6, 17–20]. So, one may assume that an increase in the dislocation yield limit of the NiTi-based alloys allows for improving thermal cycling stability because it suppresses an increase in dislocation density during thermal cycling. To increase the dislocation yield limit, the alloys are subjected to various hardening processes such as preliminary training (thermal cycling under or without stress through a temperature range of the martensitic transformations), precipitation hardening (on annealing of Ni-rich NiTi alloys), grain refinement (by severe plastic deformation and post-deformation annealing), solid solution hardening (by adding of ternary or more elements in the NiTi alloy), or preliminary deformation [3, 20–21]. The results showed that in some cases, after hardening, the thermal cycling stability of the transformation temperatures improves; however, in most cases, such studies were carried out on thermal cycling without stress. At the same time, in applications, the shape memory alloy element is subjected to cooling and heating under constant stress or under an actuator regime when the

stress varies on cooling and heating. In this case, the question arises whether the alloys showing good thermal cycling stability during thermal cycling without stress remain the same during thermal cycling under stress.

One may assume that the dislocation density variation during thermal cycling under stress is larger than without stress. Hence, the thermal cycling stability of the transformation temperatures should be worse than without stress. On the other hand, the alloy hardening that improves the thermal cycling stability of the martensitic transformation during thermal cycling without stress can maintain it during thermal cycling under stress. This question is very important from the application point of view because it helps to choose the NiTi-based alloys that demonstrate stable properties in devices. At the same time, the fundamental meaning of this problem is also crucial because it allows us to study the relation between the yield limit for dislocation slip and the variation in the functional properties of the NiTi-based alloys during thermal cycling. This paper aimed to study the thermal cycling stability of the martensitic transformation temperatures during thermal cycling without or under constant stress in the NiTi-based alloys. To clarify how the alloy hardening affects the thermal cycling stability of the martensitic transformation temperature, five Ti-Hf-Ni-Cu alloys with various yield limits for dislocation slip were studied in the paper.

2. Methods

The Ti-Hf-Ni-Cu alloys with various chemical compositions (given in Table 1) were produced in a vacuum arc furnace under an argon atmosphere purified by a Ti getter. High-purity chemical elements (99.9 wt.%) were used as raw materials. Each ingot with a mass of 20 g and a diameter of 20 mm was turned over and remelted five times to obtain a homogeneous composition. The concentrations of Ti, Hf, Ni and Cu elements were different in the alloys. However, the concentrations of Ti+Hf and Ni+Cu groups were constant and equal to 50.2 at.% and 49.8 at.%, respectively. For convenience, the alloys were labeled by the concentration of Hf and Cu (see Table 1).

Table 1. The chemical composition of the billets.

Alloy	Label	Chemical composition, at.%			
		Ti	Hf	Ni	Cu
$Ti_{49.2}Hf_1Ni_{48.8}Cu_1$	Hf1-Cu1	49.2	1	48.8	1
$Ti_{49.2}Hf_1Ni_{44.8}Cu_5$	Hf1-Cu5	49.2	1	44.8	5
$Ti_{40.7}Hf_{9.5}Ni_{48.8}Cu_1$	Hf9.5-Cu1	40.7	9.5	48.8	1
$Ti_{40.7}Hf_{9.5}Ni_{44.8}Cu_5$	Hf9.5-Cu5	40.7	9.5	44.8	5
$Ti_{40.7}Hf_{9.5}Ni_{39.8}Cu_{10}$	Hf9.5-Cu10	40.7	9.5	39.8	10

The structure of these alloys, the martensitic transformations and mechanical properties were previously studied, and results were published in [22]. All alloys include the Ti-Hf-Ni-Cu matrix and the $(Ti, Hf)_2(Ni, Cu)$ particles, the volume fraction of which was not larger than 3% and was hardly affected by the alloy composition. The Ti-Hf-Ni-Cu matrix undergoes the martensitic transformation from the austenite cubic B2 phase to the martensite monoclinic B19' phase on cooling and the B19'→B2 transformation on heating at temperatures shown in Table 2. The minimum yield limit for dislocation slip (determined on tension in the austenite state) was found in the Hf1-Cu1 and Hf1-Cu5 alloys, which were equal to 350 ± 5 MPa. The maximum yield limit for dislocation slip of 740 MPa was observed in the Hf9.5-Cu10 alloy.

The ingots were cut (by electro-discharge machine) to the plates with a thickness of 0.8 mm, which was used to cut the sample with a size of 3 mm × 3 mm for thermal cycling without stress. The plates with the same thickness were used to cut the dog-bone samples (working length of 7 mm, width of 1 mm) for thermal cycling under stress (Fig. 1). Ten thermal cycles without stress (free thermal cycles) were carried out in differential scanning calorimeter (Mettler Toledo) in a temperature range A_f + 30°C to M_f −30°C with a cooling heating rate of 10°C/min.

To carry out ten thermal cycles under stress, the dog-bone samples were installed on the inter-grippers, which were fixed in the standard grippers of the Shimadzu testing machine equipped with a thermal chamber. The samples were heated to a temperature of A_f +50°C, loaded to stress σ and subjected to cooling and heating under stress ten times. The temperature of the samples was measured by a micro-thermocouple attached to the sample surface and isolated by the asbestos rod. The strain variation on cooling and heating under stress was measured by video-extensometer according to standard procedure. The value of stress σ was chosen as 100 MPa for the Hf1-Cu1 and Hf1-Cu5 alloys and 200 MPa for the Hf9.5-Cu1, Hf9.5-Cu5 and Hf9.5-Cu10 alloys.

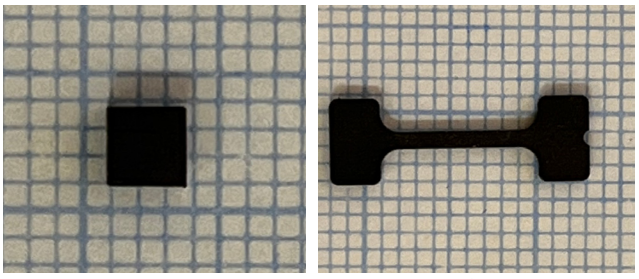

a b

Fig. 1. Samples used for thermal cycling without stress (a) and under stress (b). The background is the paper with a 1 mm grid.

Table 2. Temperatures of the martensitic transformations (M_s and M_f are the start and finish temperature of the forward B2→B19' transformation; A_s and A_f are the temperatures of the reverse B19'→B2 transformation) and the mechanical behaviour measured during tension in the austenite state (σ_d — dislocation yield limit; ε_{max} — maximum strain up to failure measured in the austenite state).

Alloy	Temperatures of the B2↔B19' martensitic transformation	Mechanical behaviour
Hf1-Cu1	M_s = 86°C, M_f = 34°C, A_s = 69°C, A_f = 110°C	σ_d = 350 MPa, ε_{max} = 4.6 %
Hf1-Cu5	M_s = 61°C, M_f = 19°C, A_s = 41°C, A_f = 83°C	σ_d = 350 MPa, ε_{max} = 10 %
Hf9.5-Cu1	M_s = 107°C, M_f = 60°C, A_s = 116°C, A_f = 169°C	σ_d = 480 MPa, ε_{max} = 5.4 %
Hf9.5-Cu5	M_s = 86°C, M_f = 35°C, A_s = 97°C, A_f = 152°C	σ_d = 580 MPa, ε_{max} = 2.4 %
Hf9.5-Cu10	M_s = 55°C, M_f = 5°C, A_s = 38°C, A_f = 99°C	σ_d = 740 MPa, ε_{max} = 1.7 %

The stress value was chosen to provide a large recoverable strain and a small irrecoverable strain. Cooling and heating of the Hf1-Cu1 and Hf1-Cu5 alloys under 200 MPa was accompanied by a large irrecoverable strain, which was why the stress for these alloys was chosen as 100 MPa. At the same time, the alloys with an Hf concentration of 9.5 at.%, demonstrating a small recoverable strain on cooling and heating under 100 MPa, thus prompting the selection of a 200 MPa stress level for these alloys.

3. Results

Figure 2a shows the calorimetric curves found in the Hf9.5-Cu1 alloy in the first, fifth and tenth cycles. It is seen that a heat release peak is observed during cooling due to the forward B2→B19' transformation, and a heat absorption peak is found during heating due to the reverse B19'→B2 transformation. The peaks shift to lower temperatures as the number of thermal cycles increases. It is seen that the variation in the transformation temperature during the first five cycles was significantly larger than during the next five cycles.

The temperatures of the martensitic transformations were determined according to ASTM standards, and their dependences on the thermal cycle number are given in Fig. 2b–f. It is seen that the transformation temperatures decrease with increasing thermal cycle number. Presumably, the temperatures in the Hf9.5-Cu10 alloy appear to be stable; however, it is observed only in the first ten cycles; subsequent cycling leads to a decrease in all temperatures (see in [23] where the variation in transformation temperatures during 500 thermal cycles is shown in Hf9.5-Cu10 alloy). Nevertheless, during the first ten thermal cycles, a large variation in transformation temperatures was observed in the Hf1-Cu1 (Fig. 2b), Hf9.5-Cu1 (Fig. 2d) and Hf9.5-Cu5 (Fig. 2e) alloys. The Hf1-Cu5 and Hf9.5-Cu10 alloys showed a small variation in the transformation temperatures, so one may expect these two alloys must demonstrate stable functional properties during 10 thermal cycles under stress.

Figure 3a shows the strain vs temperature curves obtained in the Hf1-Cu5 alloy during thermal cycling under 100 MPa in the 1st, 5th and 10th cycles. It is seen that the strain accumulates during cooling due to the forward B2→B19' transformation, and it recovers during heating due to the reverse B19'→B2 transformation. The strain recovery during heating was not complete in each cycle, which led to the ε(*T*) curve shifting up during thermal cycling under stress. Moreover, the ε(*T*) curves shift to lower temperatures due to a decrease in the temperatures of the martensitic transformation during thermal cycling. Using the ε(*T*) curves for each cycle, the transformation temperatures (M_s, M_f, A_s, A_f), as well as the value of the shape memory effect (ε^{SM}) and irrecoverable strain (ε_{ir}), were measured as shown in Fig. 3b. The variations in the transformation temperatures during thermal cycling under stress measured in Hf1-Cu1 and Hf1-Cu5 alloys are shown in Figs. 3c,d. It is seen that all temperatures decrease during thermal cycling under 100 MPa. The value of the shape memory effect increased during thermal cycling under 100 MPa due to the training effect (Fig. 3e). The irrecoverable strain decreased during thermal cycling of the Hf1-Cu1 alloy, and this parameter was constant in the Hf1-Cu5 alloy (Fig. 3f).

Figure 4a shows the ε(*T*) curves found in the Hf9.5-Cu1 alloy during the 1st, 5th and 10th thermal cycling under 200 MPa. It is seen that the ε(*T*) curves changes during thermal cycling under 200 MPa as in the Hf1-Cu5 alloys shown in Fig. 3a. The transformation temperatures changed during thermal cycling under 200 MPa differently. In the Hf9.5-Cu1 and

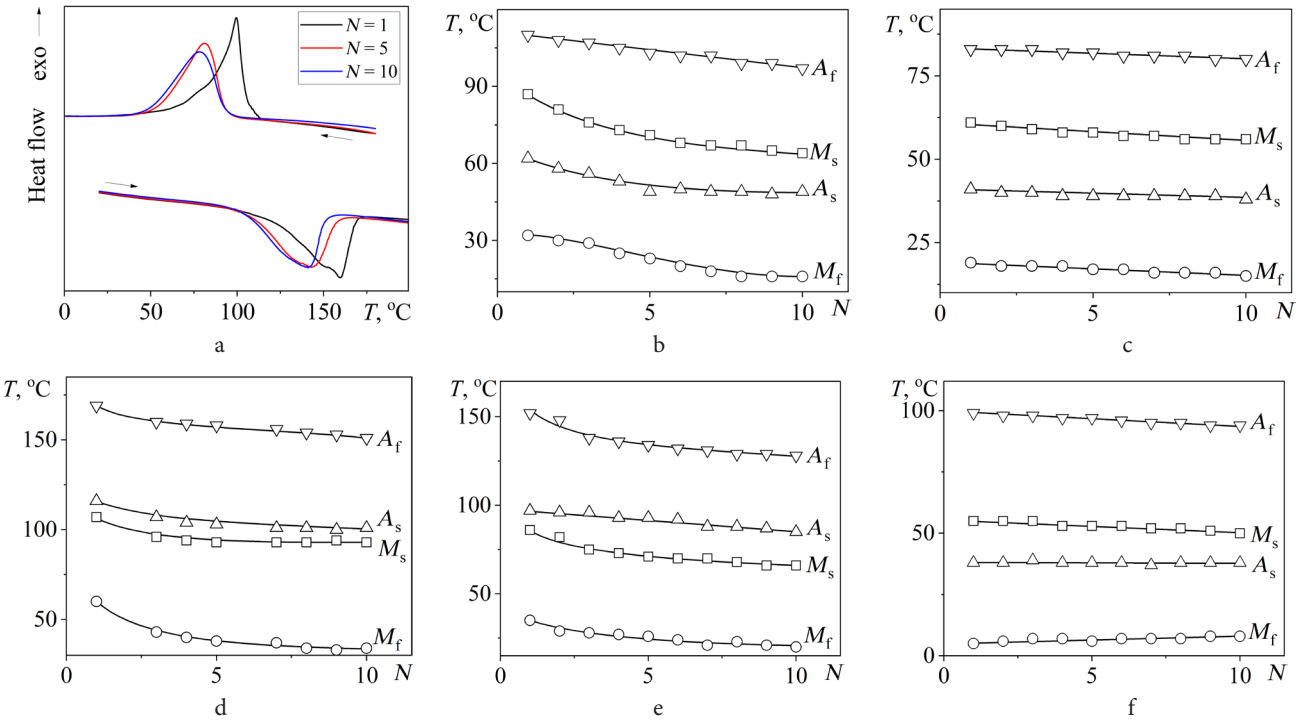

Fig. 2. (Color online) Calorimetric curves measured in the 1st, 5th and 10th cycles for Hf9.5-Cu1 alloy (a). The dependences of the martensitic transformation temperatures on thermal cycle number measured in Hf1-Cu1 (b), Hf1-Cu5 (c), Hf9.5-Cu1 (d), Hf9.5-Cu5 (e) and Hf9.5-Cu10 (f) alloys.

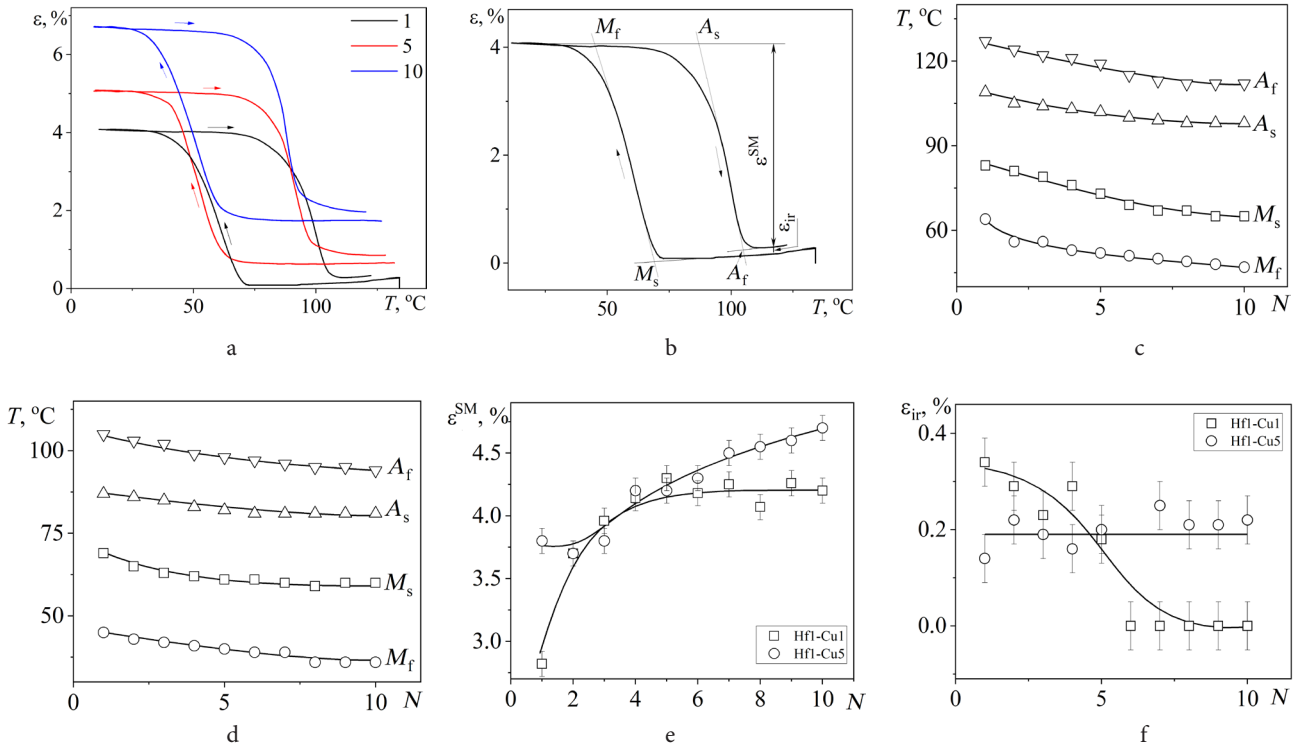

Fig. 3. (Color online) The strain vs temperature curves obtained in the 1st, 5th and 10th thermal cycles under 100 MPa in the Hf1-Cu5 alloy (a). The scheme for determining the transformation temperatures, the value of the shape memory effect and irrecoverable strain (b). The variation in the transformation temperatures during thermal cycling under 100 MPa found in the Hf1-Cu1 (c) and Hf1-Cu5 (d) alloys. The variation in the value of the shape memory effect (e) and irrecoverable strain (f) during thermal cycling under a stress of 100 MPa.

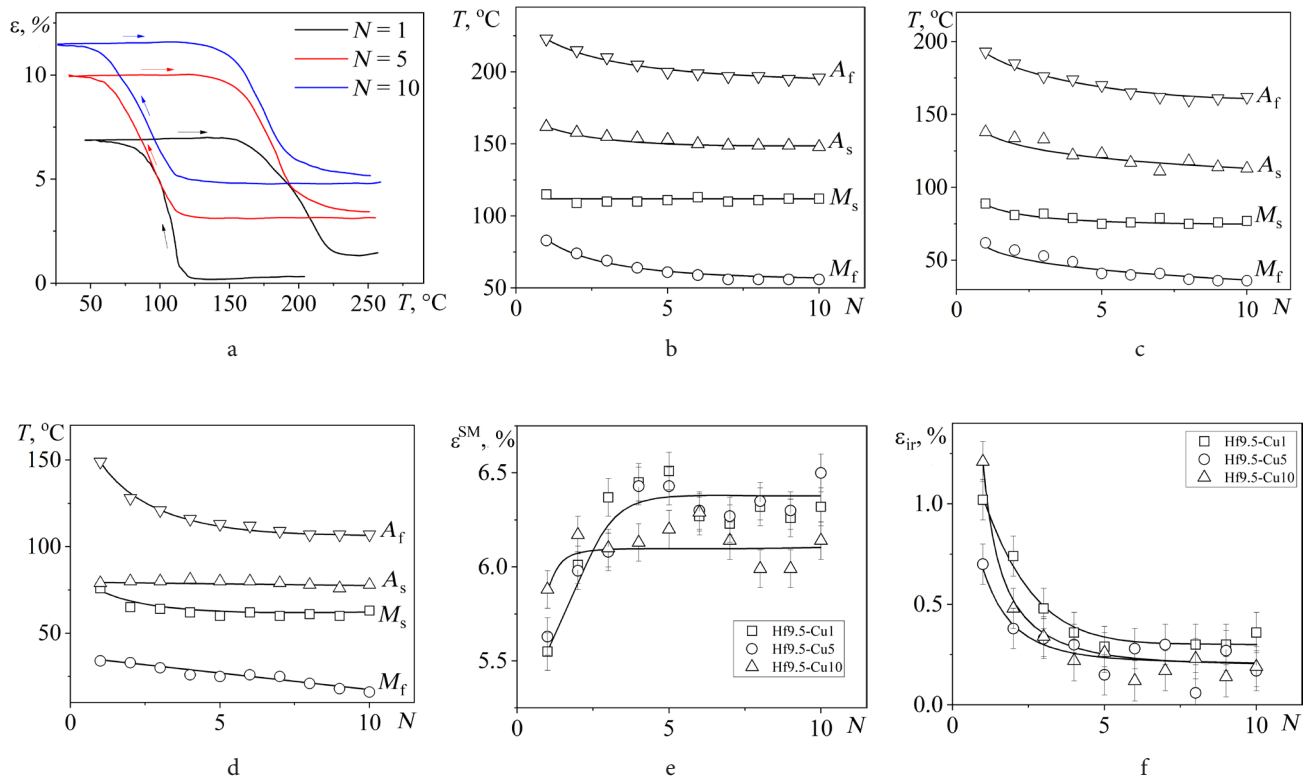

Fig. 4. (Color online) The strain vs temperature curves obtained in the 1st, 5th and 10th thermal cycles under 200 MPa in the Hf9.5-Cu1 alloy (a). The variation in the transformation temperatures during thermal cycling under 200 MPa found in the Hf9.5-Cu1 (b), Hf9.5-Cu5 (c) and Hf9.5-Cu10 (d) alloys. The variation in the value of the shape memory effect (e) and irrecoverable strain (f) during thermal cycling under a stress of 200 MPa.

Hf9.5-Cu10 alloys, the M_s and A_s temperatures varied less than the A_f and M_f temperatures (Fig. 4 b, d). In the Hf9.5-Cu5 alloy, all transformation temperatures decreased during thermal cycling under 200 MPa with a close rate (Fig. 4 c). The value of the shape memory effect hardly depended on the Cu concentration in the alloys with 9.5 at.% of Hf. During thermal cycling, it slightly increased due to the training effect, and it became equal to 6.25 ± 0.25% starting the fifth cycle (Fig. 4 e). The irrecoverable strain was maximum in the first cycle and significantly decreased during thermal cycling. The larger the Cu concentration in the alloys with 9.5 at.% of Hf, the more intensive is a decrease in irrecoverable strain during thermal cycling under 200 MPa.

Table 3 shows the $\Delta M_s = M_s^1 - M_s^{10}$, $\Delta M_f = M_f^1 - M_f^{10}$, $\Delta A_s = A_s^1 - A_s^{10}$, $\Delta A_f = A_f^1 - A_f^{10}$ values, which were determined for cycles carried out without or under stress. If the variation in transformation temperatures during thermal cycling under stress was larger than without stress, then this position is filled by red. If the stress did not influence the variation in the transformation temperatures during thermal cycling, these cells are filed by yellow. If the variation in the transformation temperatures on stress was less than without stress, then these positions were filled by green. Table 3 shows no common effect of the stress on the variation in the transformation temperatures in the Ti-Hf-Ni-Cu alloys during thermal cycling. For instance, in Hf1-Cu1, the variation in the M_f, A_s and A_f temperatures during thermal cycling under stress was the same as without stress. In the Hf1-Cu5 alloy, the variation in the transformation temperatures during thermal cycling under stress was larger than without stress. In Hf9.5-Cu1 and Hf9.5-Cu5 alloys, the variation in the M_s temperature on thermal cycling under stress was less than without stress. Moreover, the alloys demonstrating the stable martensitic transformation temperatures during free thermal cycling (Hf1-Cu5 and Hf9.5-Cu10) did not keep it under thermal cycling under stress. In both alloys, the variation in the transformation temperatures during thermal cycling under stress was significantly larger than without stress; however, they remained less than the variation in the transformation temperatures in other alloys. The exception was the variation in the A_f temperature in the Hf9.5-Cu10 alloy, which was the largest compared to all the alloys.

4. Discussion

It is known that the M_s and A_f temperatures are determined by the transformation hysteresis and the stress state, while the M_f and A_s temperatures are additionally effected by the elastic energy stored during the martensitic transformation. It is unclear which parameters (stress, defect density, type of martensitic transformation) affect the stored elastic energy. So, to avoid the analyses of the influence of the stored elastic energy on the variation in transformation temperatures during thermal cycling under stress, the M_f and A_s temperatures were excluded from the discussion. Thus, the reasons for the variations in the M_s and A_f temperatures during thermal cycling under stress were discussed as compared to identical ones observed during free thermal cycling.

To characterize the difference in the variation in the M_s and A_f temperatures during thermal cycling under stress compared to free thermal cycling, the $\Delta_s = (\Delta M_s^\sigma - \Delta M_s^0)/\Delta M_s^0$ and $\Delta_f = (\Delta A_f^\sigma - \Delta A_f^0)/\Delta A_f^0$ values were determined, where the ΔM_s^0 and ΔA_f^0 were the variation in these temperatures during 10 free thermal cycles and ΔM_s^σ and ΔA_f^σ values were the variations during 10 thermal cycled under a stress of 100 MPa for Hf1-Cu1 and Hf1-Cu5 alloys or 200 MPa for the Hf9.5-Cu1, Hf9.5-Cu5 and Hf9.5-Cu10 alloys (taken from Table 3). The Δ_s and Δ_f values are shown in Fig. 5, where the positive value means that the variation in the M_s or A_f temperature during thermal cycling under stress was larger than without stress. In contrast, the negative value shows that the variation in these temperatures under stress was less than without stress.

As mentioned above, it is believed that an increase in the dislocation density causes variation in the transformation temperatures during thermal cycling. So, one may expect that in the alloy with the highest yield limit for the dislocation slip, the variation in the dislocation density during thermal cycling must is less than in the alloy with the lowest σ_d value. In this case, the Hf9.5-Cu10 alloy with the highest σ_d value must demonstrate less variation in the transformation temperatures during thermal cycling than the Hf9.5-Cu1

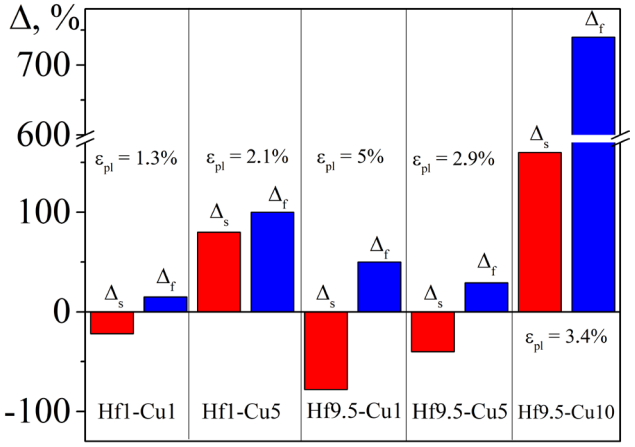

Fig. 5. (Color online) The $\Delta_s = (\Delta M_s^\sigma - \Delta M_s^0)/\Delta M_s^0$ and $\Delta_f = (\Delta A_f^\sigma - \Delta A_f^0)/\Delta A_f^0$ values as well as the plastic strain measured in the 10th thermal cycle under stress. The stress was equal to 100 MPa for the Hf1-Cu1 and Hf1-Cu5 alloys and 200 MPa for other alloys.

Table 3. (Color online) Variation in the transformation temperatures during 10 thermal cycles without or under stress.

Alloy	Hf1-Cu1		Hf1-Cu5		Hf9.5-Cu1		Hf9.5-Cu5		Hf9.5-Cu10	
Stress σ, MPa	0	100	0	100	0	200	0	200	0	200
ΔM_{ss}, °C	−23	−18	−5	−9	−14	−3	−20	−12	−5	−13
ΔM_{fs}, °C	−16	−17	−4	−8	−26	−27	−15	−26	+3	−18
ΔA_{ss}, °C	−13	−11	−3	−6	−15	−14	−12	−25	0	−1
ΔA_{fs}, °C	−13	−15	−3	−6	−18	−27	−24	−31	−5	−42

alloy, the σ_d value of which was 1.5 times less than in the Hf9.5-Cu10 alloy. This is observed in free thermal cycling (Table 3). At the same time, this assumption is not confirmed by the experimental data during thermal cycling under stress. The variation in the M_s and A_f temperatures during thermal cycling under stress in the Hf9.5-Cu10 alloy was larger than in the Hf9.5-Cu1 alloy (Table 3). Moreover, stress leads to a huge intensification in the variation in the transformation temperatures in the Hf9.5-Cu10 alloy during thermal cycling (Fig. 5) and Δ_s and Δ_f values were equal to 120 and 740%. Therefore, the results of the present paper contradict the assumption that the minimum variation in the transformation temperatures during thermal cycling must be observed in the alloys with the heist dislocation yield limit. Thus, there is no relation between the σ_d value and the decreasing rate of the transformation temperatures. This is confirmed by the data found for the alloys with 1 at.% of Hf atoms in which the yield limit for the dislocation slip was the same (Table 2), while the variation in the M_s and A_f temperatures, as well as the Δ_s and Δ_f values, significantly differed.

The difference between thermal cycling without or under stress is because the non-oriented martensite formed in the first case of cooling, and the mixture of the oriented and non-oriented martensite appears in the second case. The formation of the oriented martensite is accompanied by high internal stress. One may assume that this leads to a significant increase in the dislocation density during thermal cycling under stress. Thus, the different variations in transformation temperatures during thermal cycling under or without stress may be due to a larger variation in dislocation density during the formation of oriented martensite.

The variation in dislocation density may be estimated by the value of the irreversible plastic strain. It is well-known that the variation in dislocation density during thermal cycling under stress is the reason for accumulation of the macroscopic plastic strain. The larger the variation in the dislocation density, the larger the plastic stain, which may be estimated as the sum of the irreversible strain measured in each cycle. To clarify the relation between the dislocation density variation and the variation in the transformation temperatures during thermal cycling under stress, the plastic strain accumulated during 10 thermal cycles and the Δ_s and Δ_f values were shown together in Fig. 5. It is seen in alloys with 1 at.% of Hf atoms, an increase in the plastic strain from 1.3% in Hf1-Cu1 alloys to 2.1% in Hf1-Cu5 alloy increases the Δ_f value and changes the Δ_s value from negative to positive. At the same time, an increase in the plastic strain from 3.4% in Hf9.5-Cu10 alloys to 5% in Hf9.5-Cu1 alloy decreases both Δ_s and Δ_f values. So, there is no correlation between the plastic strain accumulated during thermal cycling under stress and the variation in the transformation temperatures. Thus, one may conclude that the different variation in the transformation temperature during thermal cycling under stress compared to free thermal cycling is not caused by the variation in dislocation density.

Therefore, the variation in transformation temperatures in thermal cycling under stress may be higher, lower, or the same as during free thermal cycling. Thus, there is no reason to choose an alloy showing stable martensitic transformation on free thermal cycling for applications where the shape memory element is subjected to thermal cycling under stress. The intensity of the variation in the transformation temperatures during thermal cycling under stress compared to free thermal cycling did not depend on the chemical composition, yield limit for dislocation slip or the dislocation density.

5. Conclusions

The results of the study may be summarized as follows:

1. The stability in the temperatures of the B2 ↔ B19' martensitic transformation during thermal cycling without stress is not maintained during thermal cycling under stress in the Ti-Hf-Ni-Cu alloys with various chemical compositions.
2. The variation in the transformation temperatures during thermal cycling under stress may be the same, smaller or larger than during free thermal cycling.
3. The variation in different martensitic transformation temperatures (M_s, M_f, A_s, A_f) during thermal cycling under stress may be positive or negative in the same alloy. For instance, in the $Ti_{40.7}Hf_{9.5}Ni_{48.8}Cu_1$, the variation in the M_s temperatures during thermal cycling under stress was less than without stress. However, the variation in the A_f temperature during thermal cycling under stress was larger than without stress. The variation in the A_s and M_f temperatures did not depend on whether the stress was applied to thermal cycling.
4. The intensification in the transformation temperatures variation during thermal cycling under stress compared to free thermal cycling did not depend on the chemical composition of the alloy, yield limit for dislocation slip or variation in the dislocation density. This showed that the variation in the dislocation density is not the main reason for the variation in the transformation temperatures during thermal cycling.

References

1. J.M. Jani, M. Leary, A. Subic, M.A. Gibson, A review of shape memory alloy research, applications and opportunities, Mater Design 56 (2014) 1078–1113.
2. R.A. Abubakar, F. Wang, L. Wang, A review on Nitinol shape memory alloy heat engines, Smart Mater. Struct. 30 (2021) 013001.
3. S. Miyazaki, Y. Igo, K. Otsuka, Effect of thermal cycling on the transformation temperatures of Ti-Ni alloys, Acta Metall. 34 (1986) 2045–2051.
4. P.G. McCormick, Y. Liu, Thermodynamic analysis of the martensitic transformation in NiTi-II. Effect of transformation cycling, Acta Metall. Mater. 42 (1994) 2407–2413.
5. N. Resnina, S. Belyaev, Multi-stage martensitic transformations induced by repeated thermalcycling of equiatomic TiNi alloy, J. Alloys Compd. 486 (2009) 304–308.
6. A.R. Pelton, G.H. Huang, P. Moine, R. Sinclair, Effects of thermal cycling on microstructure and properties in Nitinol, Mater. Sci. Eng. A 532 (2012) 130–138.
7. Y. Furuya, Y.C. Park, Thermal cyclic deformation and degradation of shape memory effect in Ti-Ni alloy, Nondestr. Test. Eval. 8–9 (1992) 541–554.

8. Y. Li, X. Mi, B. Gao, Effects of thermomechanical cycling on the shape memory behavior and transformation temperatures of a Ni50.2Ti49.8 alloy, J. Tan Rare Metals 27 (2008) 522 – 525.
9. C. N. Saikrishna, K. V. Ramaiah, S. Allam Prabhu, S. K. Bhaumik, On stability of NiTi wire during thermo-mechanical cycling, Bull. Mater. Sci. 32 (2009) 343 – 352.
10. X. M. He, L. Z. Zhao, X. M. Wang et al., Transformation behaviour with thermal cycling in $Ti_{50}Ni_{43}Cu_7$ shape memory alloy, Mater. Sci. Eng. A 427 (2006) 327 – 330.
11. S. H. Kang, H. J. Im, H. W. Lee, T. H. Nam, Changes in Martensitic Transformation Temperatures during Thermal Cycling in Ti-Ni-Zr Shape Memory Alloys, Metals Mater. Intern. 7 (2001) 201 – 205.
12. S. Besseghini, E. Villa, A. Tuissi, Ni-Ti-Hf shape memory alloy: effect of aging and thermal cycling, Mater. Sci. Eng. A 273 – 275 (1999) 390 – 394.
13. J. Pang, J. Tian, P. Dang et al., Attainment of large thermal hysteresis and good thermal cyclic stability in multi-component TiHfZrNi alloys, Scripta Mater 249 (2024) 116164.
14. S. Baradari, N. Resnina, S. Belyaev, Nili-Ahmadabadi M., Cyclic Stability of $Ni_{44.8}Cu_5Ti_{45.2}Hf_5$ and Zr-Substituted $Ni_{44.8}Cu_5Ti_{40.2}Hf_5Zr_5$ Medium-Entropy Shape Memory Alloys, Adv. Eng. Mater. 24 (2022) 2200106.
15. S. Baradari, N. Resnina, S. Belyaev, M. Nili-Ahmadabadi, Martensitic phase transformation and shape memory properties of the as-cast NiCuTiHf and NiCuTiHfZr alloys, J. Alloys Compd. 888 (2021) 161534.
16. S. P. Belyaev, N. N. Resnina, A. I. Bazlov et al., Thermal cycling stability of the B2↔B19' transformation in the Ti-Hf-Ni-Cu alloys with cast and ultrafine-grained structures, Lett. Mater. 15 (2025) 8 – 14.
17. J. Zhang, C. Somsen, T. Simon et al., Leaf-like dislocation substructures and the decrease of martensitic start temperatures: A new explanation for functional fatigue during thermally induced martensitic transformations in coarse-grained Ni-rich Ti-Ni shape memory alloys, Acta Mater. 60 (2012) 1999 – 2006.
18. M. Coduri, A. Lausi, A. Tuissi, The High Performance Shape Memory Effect (HP-SME) in Ni Rich NiTi Wires: In Situ X-Ray Diffraction on Thermal Cycling, MATEC Web Conf. 33 (2015) 03008.
19. A. Churakova, D. Gunderov, Increase in the dislocation density and yield stress of the $Ti_{50}Ni_{50}$ alloy caused by thermal cycling, Mater. Today: Proc. 4 (2017) 4732 – 4736.
20. Y. X. Tong, B. Guo, F. Chen et al., Thermal cycling stability of ultrafine-grained TiNi shape memory alloys processed by equal channel angular pressing, Scripta Mater 67 (2012) 1 – 4.
21. A. Churakova, E. Kayumova, D. Gunderov, D. Magomedova, Interrelation of microstructure and kinetics of martensitic transformations in TiNi alloy in different structural states under thermal cycling conditions, AIP Conf. Proc. 2533 (2022) 020049.
22. S. Belyaev, N. Resnina, A. Bazlov et al., Influence of the Cu and Hf concentrations on martensitic transformation, mechanical and functional behaviour of the Ti-Hf-Ni-Cu shape memory alloys, Trans. Indian Inst. Metals 78 (2025) 138.
23. N. N. Resnina, S. P. Belyaev, A. I. Bazlov et al., Thermal cycling stability of the martensitic transformation in Ti40.7Hf9.5Ni49.8–xCux (x = 1, 5 or 10 at.%) cast alloys, Mater. Phys. Mech. 53 (2025) 57 – 67.